PROCEEDINGS OF SCIENCE

Studying $WW\gamma$ and $WZ\gamma$ production in proton–proton collisions at $\sqrt{s}$ = 8 TeV with the ATLAS experiment

Julia Isabell Djuvsland*, **on behalf of the ATLAS Collaboration**
Ruprecht-Karls-Universität Heidelberg (DE)
E-mail: julia.djuvsland@cern.ch

Measuring triboson final states at the Large Hadron Collider provides a test of the non-Abelian structure of the Standard Model of particle physics. This structure gives rise to self-interactions of the electroweak gauge bosons and the Standard Model predicts the exact strength of these couplings. Any observed deviation from these expectations would imply the existence of new physical phenomena.

These proceedings present a study of triboson production using $WW\gamma$ and $WZ\gamma$ events produced in proton–proton collisions corresponding to an integrated luminosity of 20.2 fb^{-1} at a centre-of-mass energy of $\sqrt{s} = 8$ TeV and recorded with the ATLAS detector. The $WW\gamma$ production cross-section is measured using the fully-leptonic final state containing an electron, a muon and a photon. Furthermore, upper limits on the production cross-section of the fully-leptonic final state and semi-leptonic final states containing an electron or a muon, two jets and a photon are derived. In addition, upper limits on the production cross-section are derived in a phase space optimised for the search of physics beyond the Standard Model. The limits are computed for all final states individually and for the combination of the electron and muon channel of the semi-leptonic final states. The results obtained in this phase space are combined and interpreted as confidence intervals on anomalous quartic gauge couplings using an effective field theory.

PoS(EPS-HEP2017)755

ATL-PHYS-PROC-2017-164
29/09/2017

The European Physical Society Conference on High Energy Physics
5-12 July
Venice, Italy

*Speaker.

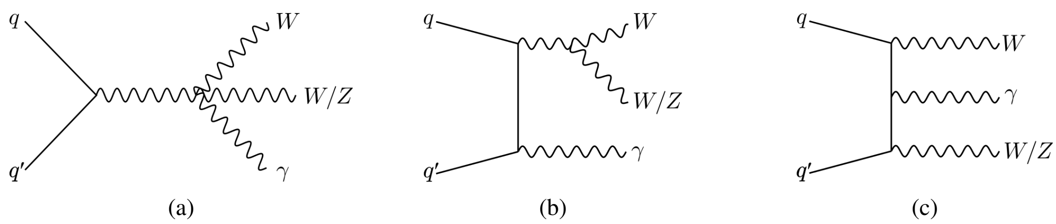

Figure 1: Feynman diagrams of $WV\gamma$ production. Figure (a) shows the diagram including the quartic vertex, while Figures (b) and (c) show the the production including radiative processes. From Reference [7].

1. Introduction

The measurement of triboson final states at the LHC yields a test of the quartic gauge couplings predicted by the non-Abelian structure of the Standard Model of particle physics (SM). Since these couplings are small they have not been studied to their full extend yet and large data sets are needed. This study employs the proton–proton collisions recorded with the ATLAS detector [1] at a centre-of-mass energy of $\sqrt{s} = 8\,\text{TeV}$ and corresponding to an integrated luminosity of 20.2 fb^{-1}. The production of two heavy gauge bosons ($V = W$ or Z) in association with the massless photon (γ) is studied in three different final states:

1. the fully leptonic $e\nu\mu\nu\gamma$ channel – containing an electron, a muon, the corresponding neutrinos and a photon,
2. the semi-leptonic $e\nu jj\gamma$ channel – containing an electron, an electron neutrino, two jets and a photon,
3. the semi-leptonic $\mu\nu jj\gamma$ channel – containing a muon, a muon neutrino, two jets and a photon.

The latter two final states have been explored before [2], while the study of the fully leptonic channel extends the current results. It is only sensitive to $WW\gamma$ production, while the semi-leptonic channels study both $WW\gamma$ and $WZ\gamma$ production simultaneously. Yet, the analysis of these final states cannot distinguish $WW\gamma$ from $WZ\gamma$ events due to the limited jet energy resolution of the ATLAS detector. Four other triboson combinations have been studied at the LHC: $W\gamma\gamma$ [3, 4], $Z\gamma\gamma$ [4, 5] and WWW [6]. The full analysis of the $WV\gamma$ final states is presented in Reference [7] while in the following a shortened overview is given.

2. Analysis Strategy

The $WV\gamma$ production mode of interest contains a quartic gauge boson vertex, depicted in Figure 1a, but its detector signature cannot be distinguished from the production modes including radiative processes, shown in Figures 1b and 1c. Therefore, all production modes are considered as signal. The challenge in analysing rare processes like $WV\gamma$ production is to isolate the signal and estimate the backgrounds. The latter do not only arise from similar final states, but also from the misidentification of objects in the detector. Therefore, a mixture of data and Monte Carlo based

$e\nu\mu\nu\gamma$	$e\nu jj\gamma$ or $\mu\nu jj\gamma$
1 electron and 1 muon ($p_\mathrm{T} > 20\,\mathrm{GeV}$) with opposite charge	1 electron or 1 muon ($p_\mathrm{T} > 25\,\mathrm{GeV}$)
no 3rd lepton ($p_\mathrm{T} > 7\,\mathrm{GeV}$)	no 2nd lepton ($p_\mathrm{T} > 7\,\mathrm{GeV}$)
≥ 1 isolated photon ($E_\mathrm{T} > 15\,\mathrm{GeV}$)	≥ 1 isolated photon ($E_\mathrm{T} > 15\,\mathrm{GeV}$)
no jets ($p_\mathrm{T} > 25\,\mathrm{GeV}$)	≥ 2 jets ($p_\mathrm{T} > 25\,\mathrm{GeV}$), no b-jets
$E_\mathrm{T,rel}^\mathrm{miss} > 15\,\mathrm{GeV}$	$E_\mathrm{T}^\mathrm{miss} > 30\,\mathrm{GeV}$
$m_{e\mu} > 50\,\mathrm{GeV}$	$m_\mathrm{T} > 30\,\mathrm{GeV}$
	$70\,\mathrm{GeV} < m_{jj} < 100\,\mathrm{GeV}$

Table 1: Criteria for the definition of the $e\nu\mu\nu\gamma$, $e\nu jj\gamma$ and $\mu\nu jj\gamma$ signal regions. The missing transverse energy, $E_\mathrm{T}^\mathrm{miss}$, is computed from calibrated objects and the variable $E_\mathrm{T,rel}^\mathrm{miss}$ accounts for the angular separation of the object closest to $E_\mathrm{T}^\mathrm{miss}$ in addition.

background estimations is used and efficient selection criteria are defined. They are optimised to yield the best significance for the observation of the signal and listed in Table 1.

These selection criteria yield an expected signal purity of 45% in the $e\nu\mu\nu\gamma$ signal region. The dominant background processes are the production of top quark pairs in association with a photon ($t\bar{t}\gamma$) and Drell-Yan processes with photon radiation ($Z\gamma$). The production of WZ events can mimic the signal in case an electron is misidentified as a photon (fake γ from e). In the case that a jet is misidentified as a photon (fake γ from jets) WW and $t\bar{t}$ production can be mistakenly identified as signal.

The estimation of the fake γ from e, the fake γ from jets and the fake e from jets background contributions relies on collision data. The fake γ from e contribution is assessed by measuring the rate with which electrons are misidentified as a photons in $Z \to ee$ decays and by correcting the corresponding rate in the Monte Carlo simulations to this value. The fake γ from jets and fake e from jets background contributions are estimated simultaneously using two 2D side band methods. The methods employ three background enriched control regions each and have their signal region in common such that they can be combined using a common likelihood function. The definition of the control regions is based on the isolation energy of the electrons and photons as well as on the identification criteria of the photons and on criteria selecting events that contain electrons and jets. The estimation of all other background processes of the $e\nu\mu\nu\gamma$ final state relies on Monte Carlo simulation.

For the $e\nu jj\gamma$ ($\mu\nu jj\gamma$) final state, the selection criteria yield an expected signal purity of 2.5% (2.8%), as the background from $W\gamma$ production in association with jets ($W\gamma+$jets) is large. In these final states, sizeable contributions to the background also arise from fake γ from jets and fake ℓ from jets processes, as well as from $t\bar{t}\gamma$ production.

The estimation of the fake γ from e background contribution is done in the same way as in the $e\nu\mu\nu\gamma$ channel. The fake γ from jets, the fake ℓ from jets and the $W\gamma+$jets backgrounds are estimated simultaneously by combining three different fits: a binned maximum likelihood fit of the m_{jj} distribution, a binned maximum likelihood fit of the $E_\mathrm{T}^\mathrm{miss}$ distribution, and a 2D side band method. Through the combination, the interdependence of the different background estimation methods is accounted for. The definition of the phase spaces employed in the fits reverts the m_{jj}

requirement with respect to the signal region, such that the regions are complementary and no signal contribution has to be taken into account. The contributions of the three background components are estimated using the observed number of events in this kinematic region and their yield in the signal region is obtained by extrapolating these results using their m_{jj} distributions. All other background contributions are estimated using Monte Carlo simulation.

3. Results

The number of observed events in the $e\nu\mu\nu\gamma$ signal region exceeds the background estimation by 10.9 ± 4.1 events which corresponds to an $e\nu\mu\nu\gamma$ production cross-section of: $\sigma_{\text{fid}}^{e\nu\mu\nu\gamma} = 1.5 \pm 0.9(\text{stat.}) \pm 0.5(\text{syst.})\,\text{fb}$. This is in good agreement with the SM expectation at next-to-leading order which corresponds to $\sigma_{\text{theo}}^{e\nu\mu\nu\gamma} = 2.0 \pm 0.1\,\text{fb}$ and is computed using the VBFNLO program [8, 9, 10]. Less events than the background expectation are observed in both semi-leptonic final states and upper exclusion limits are set on their production cross-section using the CL_s method. Upper limits on the production cross-section are also determined for the $\ell\nu jj\gamma$ final state, which corresponds to the combination of the $e\nu jj\gamma$ and $\mu\nu jj\gamma$ channels. At 95% confidence level, these limits are as low as 2.5 times the expected cross-section of the SM. Figure 2 shows the photon transverse energy distribution for the three final states.

With no deviations from the SM expectation being observed, confidence intervals on anomalous quartic gauge couplings are derived. To this end, an effective field theory expanding the Lagrangian density of the SM by operators of dimension eight is employed. As unitarity can be violated in this framework, a dipole form factor [11] is used in this interpretation to counteract the effect. Anomalous quartic gauge couplings mainly lead to an increased production cross-section at high energies as can be seen by the dashed histograms in Figure 2. Thus, the sensitivity of this study is increased by raising the photon E_T thresholds (120 GeV for the $e\nu\mu\nu\gamma$ final state and 200 GeV for the $e\nu jj\gamma$ and $\mu\nu jj\gamma$ final states) and by combining all channels. Confidence intervals on the couplings strength of 14 different dimension eight operators are computed for three different values of the scale Λ_{FF} of the dipole form factor, namely ∞, 1 TeV, and 0.5 TeV. A maximum profile-likelihood ratio test statistic is employed in the limit setting that confirms and extends previous results. Furthermore, for all final states exclusion limits on the production cross-section with the raised photon E_T thresholds are computed. More details can be found in Reference [7].

4. Conclusions

The production of $WW\gamma$ and $WZ\gamma$ events is studied in $e\nu\mu\nu\gamma$, $e\nu jj\gamma$ and $\mu\nu jj\gamma$ final states. The $WW\gamma$ production cross-section is determined using the $e\nu\mu\nu\gamma$ final state and the combined $WW\gamma$ and $WZ\gamma$ production cross-section is constrained using the $e\nu jj\gamma$ and $\mu\nu jj\gamma$ final states. The results are interpreted in the framework of effective field theories by deriving confidence intervals for the coupling strength of 14 operators of dimension eight and three different choices for the unitarisation. All measurements are in agreement with the expectations of the SM that withstands yet another test.

PoS(EPS-HEP2017)755

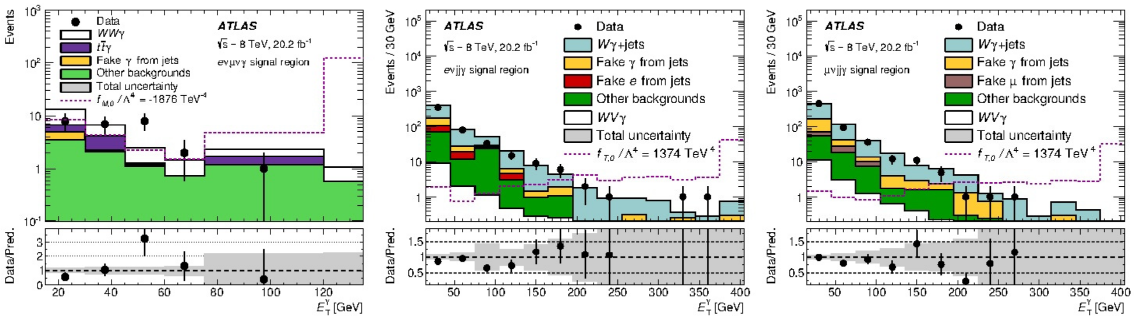

(a) $e\nu\mu\nu\gamma$ final state (b) $e\nu jj\gamma$ final state (c) $\mu\nu jj\gamma$ final state

Figure 2: Distribution of the photon transverse energy for the three final states: $e\nu\mu\nu\gamma$, $e\nu jj\gamma$, and $\mu\nu jj\gamma$. The data (round markers) are shown together with the signal and background expectations (histograms). The expected event yield for a reference model that describes physics beyond the SM is also indicated (dashed histogram); the last bin also contains overflow events. In the lower panel the ratio of the observed number of events and the sum of expected signal and background events is shown together with the the uncertainties associated with the expectations. From Reference [7].

References

[1] ATLAS Collaboration, *The ATLAS Experiment at the CERN Large Hadron Collider*, *JINST* **3** (2008) S08003.

[2] CMS Collaboration, *Search for $WW\gamma$ and $WZ\gamma$ production and constraints on anomalous quartic gauge couplings in pp collisions at $\sqrt{s} = 8$ TeV*, *Phys. Rev. D* **90** (2014) 032008.

[3] ATLAS Collaboration, *Evidence of $W\gamma\gamma$ Production in pp Collisions at $\sqrt{s} = 8$ TeV and Limits on Anomalous Quartic Gauge Couplings with the ATLAS Detector*, *Phys. Rev. Lett.* **115** (2015) 031802.

[4] CMS Collaboration, *Measurements of the* $\mathrm{pp} \to \mathrm{W}\gamma\gamma$ *and* $\mathrm{pp} \to \mathrm{Z}\gamma\gamma$ *cross sections and limits on anomalous quartic gauge couplings at $\sqrt{s} = 8$ TeV*, arXiv:1704.00366 [hep-ex].

[5] ATLAS Collaboration, *Measurements of $Z\gamma$ and $Z\gamma\gamma$ production in pp collisions at $\sqrt{s} = 8$ TeV with the ATLAS detector*, *Phys. Rev. D* **93** (2016) 112002.

[6] ATLAS Collaboration, *Search for triboson $W^{\pm}W^{\pm}W^{\mp}$ production in pp collisions at $\sqrt{s} = 8$ TeV with the ATLAS detector*, *Eur. Phys. J. C* **77** (2017) 141.

[7] ATLAS Collaboration, *Study of $WW\gamma$ and $WZ\gamma$ production in pp collisions at $\sqrt{s} = 8$ TeV and search for anomalous quartic gauge couplings with the ATLAS experiment*, *Eur. Phys. J. C* **77** (2017) 646.

[8] J. Baglio *et al.*, *Release Note - VBFNLO 2.7.0*, arXiv:1404.3940 [hep-ph].

[9] K. Arnold *et al.*, *VBFNLO: A Parton Level Monte Carlo for Processes with Electroweak Bosons – Manual for Version 2.5.0*, arXiv:1107.4038 [hep-ph].

[10] K. Arnold *et al.*, *VBFNLO: A Parton level Monte Carlo for processes with electroweak bosons*, *Comput. Phys. Commun.* **180** (2009) 1661.

[11] C. Degrande *et al.*, *Monte Carlo tools for studies of non-standard electroweak gauge boson interactions in multi-boson processes: A Snowmass White Paper*, arXiv:1309.7890 [hep-ph].